

Rev. Letters 22, 142 (1969).

<sup>23</sup>Because the single-hole states have different spin or parity than the single-particle states, and the ground state of <sup>210</sup>Pb has  $\lambda=0$ ,  $\pi=+$ , some graphs of Figs. 8 and 9 do not contribute because of general selection rules, namely 8, 9(a), and 9(b). The matrix elements corresponding to these cases are not given in Appendix IV.

<sup>24</sup>D. J. Thouless, *The Quantum Mechanics of Many-Body Systems* (Academic Press, New York, 1961).

<sup>25</sup>M. Redlich, Phys. Rev. 138, 544 (1964).

<sup>26</sup>C. T. Chen and F. W. Hurley, Nucl. Data B1, (No. 13), 1 (1966).

<sup>27</sup>We are indebted to Professor B. R. Mottelson for pointing out to us that a deficiency of the model is that our coupling Hamiltonian does not include some large matrix elements corresponding to the usual quadrupole particle-hole force.

<sup>28</sup>A. R. Edmonds, *Angular Momentum in Quantum Mechanics* (Princeton University Press, Princeton, New Jersey, 1967).

PHYSICAL REVIEW C

VOLUME 3, NUMBER 6

JUNE 1971

## Effect of the Multipole Pairing and Particle-Hole Fields in the Particle-Vibration Coupling of <sup>209</sup>Pb.

### II. The <sup>207</sup>Pb(*t,p*)<sup>209</sup>Pb Reaction at 20 MeV\*

E. R. Flynn, G. Igo,<sup>†</sup> and P. D. Barnes<sup>‡</sup>

*Los Alamos Scientific Laboratory, University of California, Los Alamos, New Mexico 87544*

and

D. Kovar

*Yale University, New Haven, Connecticut 06520*

and

D. Bes and R. Broglia<sup>§</sup>

*University of Minnesota, || Minneapolis, Minnesota 55455*

(Received 12 October 1970)

The <sup>207</sup>Pb(*t,p*)<sup>209</sup>Pb reaction has been performed at 20 MeV. The excitation of the single-particle states is used as a normalization for the distorted-wave code of Bayman and Kallio. A large number of two-particle-one-hole states are seen in the excitation region examined, the first (the  $\frac{1}{2}^-$ ) being at 2.152 MeV. The remaining states are interpreted as being multiplets of the [*p*<sub>1/2</sub><sup>-1</sup> <sup>210</sup>Pb(*J*)] configurations. The magnitudes and energy centroids of the observed states are compared with those observed in the <sup>208</sup>Pb(*t,p*)<sup>210</sup>Pb experiment and also with the theoretical treatment of a particle coupling to multipole pairing and particle-hole fields.

#### I. INTRODUCTION

The two-nucleon transfer reaction has proven to be a useful tool in the study of the properties of various nuclear states.<sup>1,2</sup> This reaction, unlike the single-nucleon transfer reaction, is sensitive to many components of the shell-model wave function. The measured two-nucleon transfer differential cross sections, for states which are built up by several components, depend strongly on the phases and magnitudes of the various configurations. Because of these properties of coherence and because the two transferred particles are highly correlated, two-nucleon transfer reactions are the specific mechanism to probe pairing fields in nuclei. However, the spectroscopic information that is obtained from this type

of reaction is not restricted only to the pairing degree of freedom. More generally, the coherence properties mentioned above imply that (*p,t*) or (*t,p*) reactions are highly selective, favoring states of the final nucleus which have a large parentage based on the target in its ground state.

There are two main purposes in doing the <sup>207</sup>Pb-<sup>209</sup>Pb experiment. The first of these is concerned with the fact that the nuclei around <sup>208</sup>Pb have been studied in detail by various direct reactions.<sup>3-5</sup> The main picture emerging from these experiments is that <sup>208</sup>Pb is a good closed-shell nucleus both in protons and neutrons and that the low-lying states of <sup>209</sup>Pb, <sup>209</sup>Bi, <sup>207</sup>Tl, and <sup>207</sup>Pb are amenable to an independent-particle shell-model description. Two nucleon transfer reactions leading to states of <sup>209</sup>Pb which have well-

established single-particle character would proceed by placing one neutron in the  $p_{1/2}$  hole and the other into the corresponding single-particle orbit above the Fermi surface. This type of transition will test the interpretation of two-nucleon transfer data, and in particular the application of distorted-wave (DW) codes for this type of reaction.

Secondly, there have recently occurred a few challenging discrepancies between the predictions of this extreme independent-particle picture and experiment. Examples of these are (a) the small value (0.6) of the spectroscopic factor associated with the  $\frac{15}{2}^-$  state at 1.4 MeV in the reactions  $^{208}\text{Pb}(t, d)$  and  $^{208}\text{Pb}(d, p)$ , and (b) the large value of the reduced transition probabilities  $B(E3; i_{13/2} \rightarrow h_{9/2})$  in  $^{209}\text{Bi}$  and  $B(E3; j_{15/2} \rightarrow g_{9/2})$  in  $^{209}\text{Pb}$ , etc. These deviations can be accounted for by the coupling of the odd particle to the 2.62-MeV octupole vibration of  $^{208}\text{Pb}$ .

It is quite natural to think that the reaction  $^{207}\text{Pb}(t, p)^{209}\text{Pb}$  can provide information about the possible coupling of pairing modes (two-particle or two-hole excitations), to the odd particle moving in the  $^{208}\text{Pb}$  core.

In a zero-order picture, only two types of states are expected to be seen in this reaction. The first of these will be the levels which are basically single particle as seen in one-nucleon stripping

studies,<sup>2</sup> these being formed by filling the  $3p_{1/2}$  hole with one neutron and placing the other into one of the single-particle orbits of  $^{209}\text{Pb}$ . The remaining type of state is the two-particle-one-hole (2p-1h) type in which the  $3p_{1/2}$  hole is left vacant and both of the transferred neutrons enter into particle orbitals. The state thus occupied would be similar to those of  $^{210}\text{Pb}$ . These states could thus be described to first order as the levels of  $^{210}\text{Pb}$  interacting with the  $3p_{1/2}$  hole and thus split into two components (when their spin differs from 0). It thus is possible to identify a number of the levels seen in this reaction by first comparing the results to single-neutron transfer studies on  $^{208}\text{Pb}$  and then to  $^{208}\text{Pb}(t, p)^{210}\text{Pb}$  results to identify the 2p-1h states. These latter states in  $^{209}\text{Pb}$  have been discussed specifically in a previous letter<sup>6</sup> and similar results at 13 MeV have also been published.<sup>7</sup>

The present results are presented in terms of absolute differential cross sections. The elastic triton cross sections were also obtained in the present experiment for use in obtaining optical-model parameters for DW calculations. Because of the sensitivity of two-nucleon stripping reactions to triton optical-model parameters the  $l=0$  transition was used to select a family of such parameters which would adequately describe  $(t, p)$  data. This result has been extended in a survey

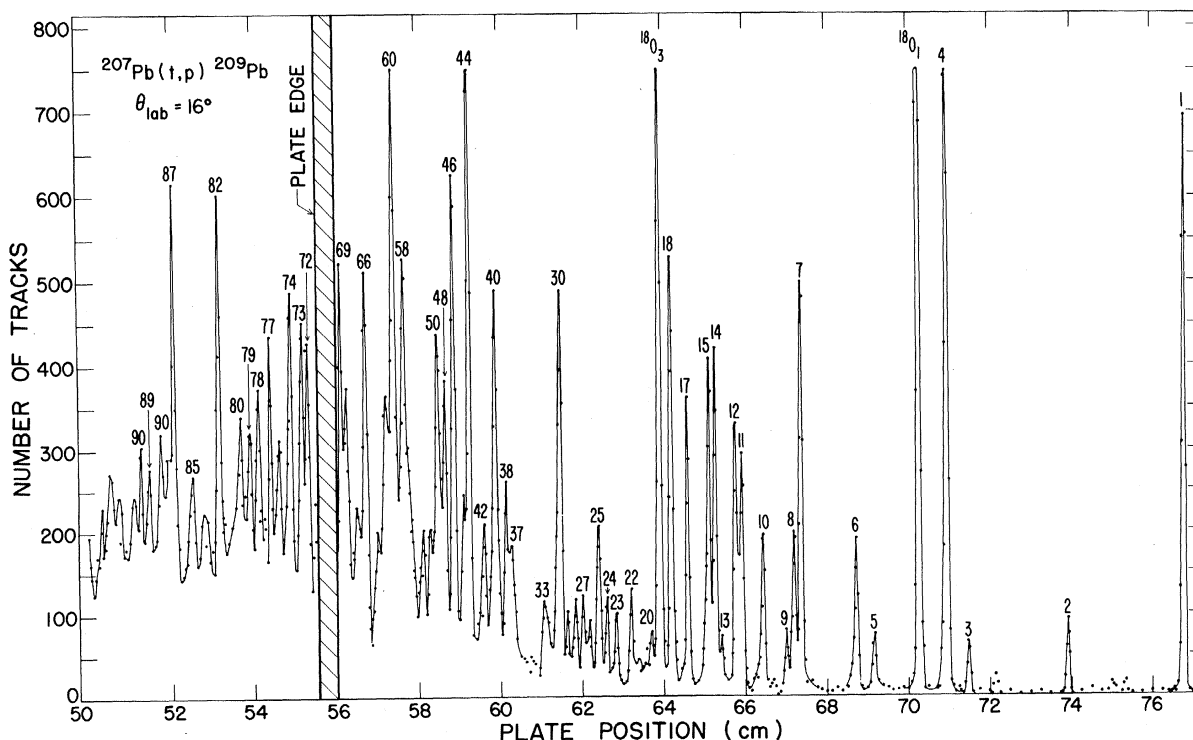


FIG. 1. Spectrum at  $16^\circ$  from spectrograph.

of elastic scattering with a particular emphasis on fitting two-nucleon stripping data.<sup>8</sup>

## II. EXPERIMENTAL TECHNIQUE

The present data were obtained by two instruments. One of these was a  $\Delta E$ - $E$  counter telescope for which data were obtained in  $3^\circ$  increments over an angular interval from  $30$  to  $72^\circ$ . The resolution of this instrument was  $32$  keV. A magnetic spectrometer of the Elbek type<sup>9</sup> was also used to obtain data at higher resolution,  $18$  keV, and over a large energy span, about  $14$  MeV of excitation. An energy spectrum covering the first  $6.5$  MeV of excitation from the spectrometer is shown in Fig. 1 for an angle of  $16^\circ$ . In all, data were obtained on this instrument at angles of  $13$ ,  $16$ ,  $20$ ,  $25$ ,  $30$ ,  $35$ ,  $40$ ,  $42$ ,  $55$ ,  $60$ , and  $63^\circ$ . Table I summarizes the energy levels seen by this and other experiments.

The object of the counter telescope data was to obtain absolute cross sections and relative normalizations for the magnetic spectrograph data. However, for the lower states the resolution was adequate to separate all of the levels and these data are included in the angular distributions. The absolute cross sections were obtained by the simultaneous measurement of the elastic scattering differential cross section which was then extended into small angles where it was Rutherford scattering. This technique has been previously employed in the lead region.<sup>3</sup> The program which performs the particle identification for the on-line computer and permits the simultaneous storage of several particles has been described elsewhere.<sup>10</sup> The spectrograph data were then normalized to these counter data by summing over the lower states for each system and then multiplying the spectrograph data by their ratio. The elastic scattering became too intense at small angles to obtain adequate statistics for the  $(t, p)$  reaction for the counter telescope and a monitor detector was used to obtain the relative spectrograph normalizations in this angular region.

## III. ELASTIC SCATTERING ANALYSIS

As mentioned previously, the elastic scattering differential cross section was measured along with the  $(t, p)$  cross sections. In addition to serving as a mechanism for obtaining the absolute cross sections for the  $(t, p)$  reaction, these data were also used to obtain optical-model parameters for use in DW calculations. For this purpose, the elastic data were extended over a larger range than the  $(t, p)$  reaction, from  $10$  to  $120^\circ$  in  $3^\circ$  intervals, so that a more exacting determination of the optical-model parameters could be made.

It is known that a large ambiguity exists in optical-model parameters for complex projectiles.<sup>11</sup> It was thus decided to find a set of such optical-model triton parameters which would fit the elastic scattering data as well as the  $(t, p)$  data.

Because of its very sharp diffractionlike pattern, the angular distribution most sensitive to the parameters describing the entrance and exit channels in a two-nucleon transfer reaction is that which is associated with an angular momentum transfer ( $L$ ) of  $0$ . For this reason, the lowest  $L=0$  transition seen in the  $^{207}\text{Pb}(t, p)^{209}\text{Pb}$  spectrum was chosen to provide a case for which the parameters put into the DW calculation could be varied until the best fit was obtained. The level at  $2153$  keV is thought to be a  $\frac{1}{2}^-$  state<sup>12</sup> and the  $(t, p)$  reaction should excite this level by an  $L=0$  transition starting from the  $\frac{1}{2}^-$  ground state of  $^{207}\text{Pb}$ . The data for this state are shown in Fig. 2 and are characteristic of an  $L=0$  transition. The proton parameters for the exit channel of the reaction were chosen from the work of Perey,<sup>13</sup> and the DW calculation itself was performed with a code due to Bayman and Kallio.<sup>14</sup> Optical-model parameters for the tritons were obtained by a search on the data using an optical-model code by Perey<sup>13</sup> and a well of the form

$$U(r) = V[1 + e^{-(r-r_0)A^{1/3}}/a_r]^{-1} + V_c + iW[1 + e^{-(r-r_0)A^{1/3}}/a_i]^{-1}, \quad (1)$$

where  $V$  and  $W$  are the depth of real and imaginary wells, respectively, and the  $r_0$ 's and  $a_\alpha$ 's are the radii and diffuseness of these wells. The real

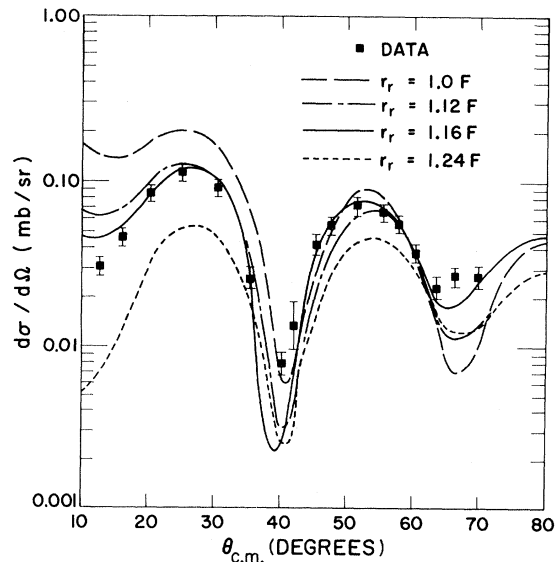


FIG. 2. Comparison of DW  $L=0$  calculations for various triton optical-model families.

TABLE I. States in  $^{209}\text{Pb}$ . The level numbers refer to states seen in the  $^{207}\text{Pb}(t,p)^{209}\text{Pb}$  reaction (see Fig. 1).

Level No.	$^{207}\text{Pb}(t,p)^{209}\text{Pb}$ (MeV)	Stripping results $^{208}\text{Pb}(t,d)^{209}\text{Pb}^a$ (MeV)	$^{208}\text{Pb}(d,p)^{209}\text{Pb}^{b-d}$ (MeV)	Pickup results $^{210}\text{Pb}(p,d)^{209}\text{Pb}^c$ (MeV)
1	0	0	0	0
2	$0.778 \pm 0.005$	0.781	$0.780^{b-d}$	0.782
3	$1.424 \pm 0.005$	1.428	$1.424^{b-d}$	1.426
4	$1.568 \pm 0.005$	1.573	$1.565^{b-d}$	1.571
5	$2.034 \pm 0.005$	2.039	$2.031^{b-d}$	2.035
6	$2.152 \pm 0.005$	2.153	$2.155^{b-d}$ $2.310^c$	2.152 2.320 2.463
7	$2.496 \pm 0.005$	2.496	$2.492^{b-d}$	2.499
8	$2.542 \pm 0.005$	2.542	$2.537^{b-d}$	2.547
9	$2.591 \pm 0.005$	2.592	$2.590^{b-d}$	2.563 2.584
10	$2.737 \pm 0.005$			2.741
11	$2.868 \pm 0.005$			2.873
12	$2.902 \pm 0.005$			2.906
13	$2.992 \pm 0.005$	2.996		
14	$3.028 \pm 0.005$			3.031
15	$3.072 \pm 0.005$			
16	$3.100 \pm 0.005$			3.077
17	$3.206 \pm 0.005$			
18	$3.309 \pm 0.005$	3.305	$3.310^{b-d}$	
19	$3.384 \pm 0.005$	3.373	$3.368^{b-d}$	
20	$3.432 \pm 0.005$			
21	$3.477 \pm 0.005$			
22	$3.561 \pm 0.005$		$3.556^{b-d}$	3.499 3.524 3.562 3.637
23	$3.659 \pm 0.005$		$3.656^{b,d}$	3.659
24	$3.708 \pm 0.005$		$3.717^c$	
25	$3.743 \pm 0.005$			3.751
26	$3.815 \pm 0.005$	3.800		3.811 3.831
27	$3.854 \pm 0.008$			
28	$3.902 \pm 0.008$		$3.905^{b-d}$	3.906
29	$3.946 \pm 0.008$		$3.942^{b-d}$	3.937
30	$3.992 \pm 0.008$	3.990	$3.985^{b-d}$	3.995
31	$4.022 \pm 0.008$		$4.021^{b-d}$	4.024
32	$4.074 \pm 0.008$	4.075	$4.075^{b,d}$	4.084
33	$4.100 \pm 0.008$	4.094	$4.095^{b,d}$ $4.113^{b,d}$	4.119
34	$4.140 \pm 0.008$	4.146	$4.138^{b-d}$	4.145
35	$4.169 \pm 0.008$		$4.175^c$ $4.216^{b,d}$	4.174 4.212
36	$4.260 \pm 0.008$			4.270
37	$4.280 \pm 0.008$			
38	$4.315 \pm 0.008$	4.322		4.315 4.345
39	$4.361 \pm 0.008$		$4.350^{b,d}$	4.358
40	$4.384 \pm 0.008$			4.395
41	$4.413 \pm 0.008$		$4.415^c$	
42	$4.451 \pm 0.008$			4.472
43	$4.508 \pm 0.008$		$4.501^c$	
44	$4.542 \pm 0.008$			4.529
45	$4.578 \pm 0.008$			4.584

TABLE I (Continued)

Level No.	$^{207}\text{Pb}(t,p)^{208}\text{Pb}$ (MeV)	Stripping results $^{208}\text{Pb}(t,d)^{208}\text{Pb}^a$ (MeV)	$^{208}\text{Pb}(d,p)^{208}\text{Pb}^{b-d}$ (MeV)	Pickup results $^{210}\text{Pb}(p,d)^{208}\text{Pb}^e$ (MeV)
46	4.632 ± 0.008			4.621
47	4.660 ± 0.008			4.671
48	4.686 ± 0.008			4.690
49	4.715 ± 0.008			4.714
50	4.731 ± 0.008			
51	4.743 ± 0.008			
52	4.754 ± 0.008			
53	4.778 ± 0.008			4.781
54	4.813 ± 0.008			4.819
55	4.843 ± 0.008			4.837
56	4.877 ± 0.008			4.865
57	4.904 ± 0.008			
58	4.931 ± 0.008			4.924 4.944
59	4.966 ± 0.010			
60	4.997 ± 0.010			
61	5.026 ± 0.010			
62	5.057 ± 0.010			
63	5.083 ± 0.010			5.074
64	5.107 ± 0.010			5.094
65	5.134 ± 0.010			5.136
66	5.161 ± 0.010			5.160
67	5.211 ± 0.010			5.222
68	5.326 ± 0.010			
69	5.241 ± 0.010			5.359
70	5.400 ± 0.010			
71	5.423 ± 0.010			
72	5.476 ± 0.010			
73	5.513 ± 0.010			
74	5.577 ± 0.010			
75	5.600 ± 0.010			
76	5.637 ± 0.010			
77	5.684 ± 0.010			
78	5.759 ± 0.010			
79	5.834 ± 0.010			
80	5.861 ± 0.010			
81	5.931 ± 0.010			
82	5.985 ± 0.010			
83	6.050 ± 0.010			
84	6.082 ± 0.010			
85	6.138 ± 0.010			
86	6.198 ± 0.010			
87	6.248 ± 0.010			
88	6.390 ± 0.010			
89	6.437 ± 0.010			

<sup>a</sup>See Ref. 3.<sup>b</sup>See Ref. 22.<sup>c</sup>See Ref. 24.<sup>d</sup>See Ref. 23.<sup>e</sup>See Ref. 21.

radius ( $r_r$ ) was held fixed and other parameters allowed to vary in each of these searches until a minimum value of  $\chi^2$  was obtained. The real radius was then set at various values between 1.0 and 1.4 F. The effect on the DW calculations for several of these optical-model families is shown in Fig. 2. For each of these sets no large effect on the quality of the fit to the elastic scattering data was seen and the value of  $\chi^2$  did not differ by more than a factor of 2. As can be seen by the figure, the best description of the  $L=0$  transfer is given by  $r_r = 1.16$  F and the resulting optical-model parameters are summarized in Table II.

The value of  $r_r = 1.16$  F has been found to give a good representation of  $L=0$  transitions for data in the region of Zr and Sn also.<sup>2</sup> Because of this, it has been used as the basis for a systematic survey of elastic scattering of tritons at 20 MeV.<sup>8</sup> The fit to the present data is included in Ref. 8.

#### IV. EXCITATION OF SINGLE-PARTICLE STATES

The single-nucleon transfer experiments using both the ( $d, p$ ) and the ( $t, d$ ) reactions have identified the levels of  $^{209}\text{Pb}$  which contain a large fraction of the single-particle strength.<sup>3</sup> These states are listed in Table III along with the spectroscopic factors obtained from Ref. 3. Figure 3 contains the results of the two-nucleon transfer DW calculations. The table shows that the seven states indicated contain almost all of the single-particle strength for the orbitals above the  $N=126$  closed shell with the exception of the  $1j_{15/2}$  level. This latter state contains only about 50% of the single-particle strength. The explanation offered for this splitting of strength is an interaction with the  $\frac{15}{2}^-$  member of the  $(103; g_{9/2}; JM)$  multiplet<sup>15</sup> expected in  $^{209}\text{Pb}$ .<sup>3, 16</sup> This interaction is expected to be strong as the matrix element

$$\langle (103; g_{9/2}; \frac{15}{2}^-) | h(03) | j_{15/2} \rangle$$

TABLE III. Single-particle states, spectroscopic factors, and two-nucleon cross sections. The factor  $N=310$  (see Ref. 18) is used in the two-body data.

$E_x$ (MeV)	One-body stripping					Two-body stripping			
	$J$	$L$	$(t, d)^a$	$(d, p)^b$	Theory <sup>c</sup>	$L$	$\left(\frac{d\sigma}{d\Omega}\right)_{\text{exp}}$	$\left(\frac{d\sigma}{d\Omega}\right)_{\text{shell model}}$	$\left(\frac{d\sigma}{d\Omega}\right)_{\text{model I}}$
0	$2g_{9/2}$	4	0.93	0.78	0.91	5	0.10	0.13	0.11
0.778	$1i_{11/2}$	6	1.05	0.96	0.98	5	0.015	0.013	0.011
1.424	$1j_{15/2}$	7	0.51	0.53	0.65	8	0.024	0.038	0.035
1.568	$3d_{5/2}$	2	0.86	0.88	0.96	3	0.130	0.175	0.154
2.034	$4s_{1/2}$	0	0.86	0.88	0.95	1	0.019	0.045	0.039
2.496	$2g_{7/2}$	4	0.90	0.78	0.97	3	0.079	0.057	0.049
2.542	$3d_{3/2}$	2	0.83	0.88	0.95	1	0.055	0.050	0.043

<sup>a</sup>See Ref. 3.

<sup>b</sup>See Ref. 23.

<sup>c</sup>See Ref. 17.

TABLE II. Optical-model parameters used in distorted-wave calculations.

	$V$	$r_r$	$a_r$	$W$	$W_d$	$r_i$	$a_i$
Triton	166.7	1.16	0.752	10.0	0.0	1.498	0.817
Proton <sup>a</sup>	53.1	1.25	0.650	0.0	17.7	1.25	0.470

<sup>a</sup>From Ref. 13.

(see Paper I<sup>17</sup>) implies no spin flip and because of the small energy separation ( $\approx 1$  MeV) between the  $(103; g_{9/2}; \frac{15}{2}^-)$  state and the  $j_{15/2}$  single-particle state.

Other single-particle states may also be mixed with  $2p-1h$  states. If we restrict these components to the basis set of states used in Paper I, the predicted spectroscopic factors are given in column 6 of Table III. The theoretical predictions are seen to agree with the experimental result that only the spectroscopic factor of the  $j_{15/2}$  deviates significantly from unity.

The ground state of  $^{207}\text{Pb}$  is well established to have a reasonably pure single-neutron character consisting of a  $3p_{1/2}$  hole.<sup>4</sup> Thus, excitation of the single-particle states of  $^{209}\text{Pb}$  by means of the  $^{207}\text{Pb}(t, p)^{209}\text{Pb}$  reaction should be describable in quite simple terms; i.e., one neutron fills the  $3p_{1/2}$  hole and the other enters the single-particle orbital. The spectroscopic amplitude for a two-nucleon stripping process, between a  $p_{1/2}$  hole and a particle state with angular momentum  $J$ , may be written

$$B(p_{1/2}J; L) = \langle J | [ (b_{p_{1/2}}^\dagger b_j^\dagger)^L b_{p_{1/2}} ]^J | 0 \rangle = \left( \frac{2L+1}{2J+1} \right)^{1/2}. \quad (2)$$

If the usual assumption is made that the two neutrons are transferred in a relative  $s$  state, then the transferred angular momentum can be determined from

$$|J - \frac{1}{2}| \leq L \leq J + \frac{1}{2}, \quad \Delta\pi = (-1)^L. \quad (3)$$

Thus, all of the single-particle states, except the  $1j_{15/2}$  level, will have odd angular momentum transfers (see Table III).

The DW program of Bayman and Kallio<sup>14</sup> is unnormalized so that an empirical normalization is required. These relatively pure single-particle states (excluding the  $1j_{15/2}$ ) offer an ideal opportunity to obtain such an empirical number and this has been exploited in a previous Letter.<sup>18</sup> In Table III (columns 8-10) the experimental cross sections are compared with the pure shell model and the model I predictions using an average normalization value of 310 obtained in Ref. 18.

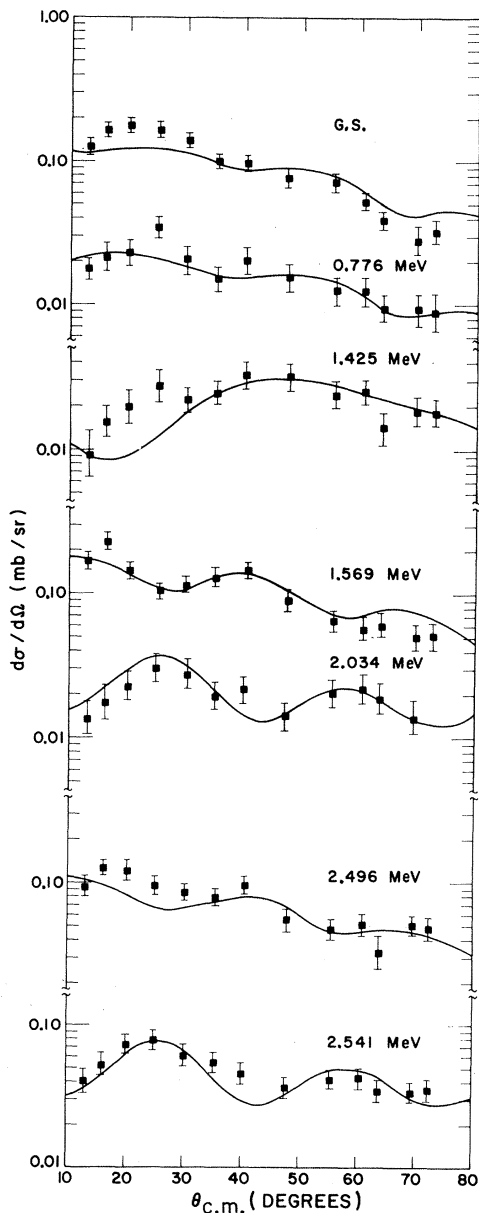


FIG. 3. DW results for the single-particle states.

*Note added in proof:* It has now been established that this value corresponds to  $c^2\nu D_0^2 = 48$  where  $c$  is the coefficient of fractional parentage for the triton-proton system,  $\nu$  is the number of identical particles in this system, and  $D_0^2$  is the overlap function.

This value was obtained by excluding the  $1j_{15/2}$  state because of its only partial single-particle character mentioned above, and also the  $4s_{1/2}$  level because of fitting difficulties. This latter state is not as well fit by the DW code, and also has an experimental angular distribution which is in disagreement with another nearby  $L=1$  transition to the  $3d_{3/2}$  state. The normalization value for the  $4s_{1/2}$  level (somewhat uncertain) is approximately 140 which is in substantial disagreement with the average value.

Although the  $1j_{15/2}$  level is the only known case where there is a significant deviation from being pure single particle, several of the other states could have additional admixtures which would affect the  $(t,p)$  transition amplitudes. The sensitivity of the two-nucleon stripping amplitude to the coherent structure of nuclear wave functions makes such reactions more dependent upon small admixtures than the single-neutron transfer; thus greater variations in the spectroscopic amplitudes for the present  $(t,p)$  reaction could occur.

In a simplified picture the transition to the  $15/2^-$  state is expected to be reduced by a factor 0.6 with respect to the single-particle estimate, i.e., if one considers the wave function for this state to consist mostly of the terms

$$|15/2^- \rangle = a |j_{15/2} \rangle + b |103; g_{9/2}; 15/2^- \rangle. \quad (4)$$

This picture implies that there is no direct transition to the unperturbed state represented by the second term. However, in a more realistic description this may be possible through the following mechanism: The reaction process introduces two particles in the states  $k$  and  $g_{9/2}$ , respectively. The first particle couples to the  $p_{1/2}$  hole creating a component of the  $\alpha=0, \gamma=3$  phonon, and therefore the second term in Eq. (4) is excited. There is only one relatively large contribution of this kind ( $k=g_{7/2}$ ) yielding a spectroscopic amplitude  $B(g_{9/2}, g_{7/2}; 8) = -0.10$ . The spectroscopic amplitude  $B(p_{1/2}, j_{15/2}; 8) = 0.80$  is a reduction by a factor 0.78 of the single-particle estimate  $\sqrt{17/16}$  of Eq. (2). The two-body transfer code indicates that the transition to a pure  $[g_{9/2}g_{7/2}]^8$  configuration is 3.8 times more intense than the transition to a  $[p_{1/2}j_{15/2}]^8$  configuration. Therefore, under the assumption that only these two (coherent) contributions are important, the total cross section is

$$\begin{aligned}\sigma &= [0.78T(p_{1/2}, j_{15/2}) \pm 0.10T(g_{9/2}, g_{7/2})]^2 \\ &= [0.78T(p_{1/2}, j_{15/2}) \pm 0.19T(p_{1/2}, j_{15/2})]^2 \quad (5) \\ &= 0.95\sigma(p_{1/2}, j_{15/2}),\end{aligned}$$

assuming the positive sign (which is verified in the more detailed calculations). Here,  $|T(i, f)|^2 = \sigma(i, f)$ . Therefore, the calculation predicts a transition rate about equal to the single-particle estimate, notwithstanding the decrease in the single-particle amplitude.

Another process which may occur is that the reaction may directly excite a pairing phonon ( $\alpha=2$ ), leaving inert the  $p_{1/1}$  hole. This would lead to a state of the type  $|n2\lambda; p_{1/2}; JM\rangle$  which may subsequently decay into the single-particle state  $|JM\rangle$ . In the  $j_{15/2}$  case, the relevant phonon in  $^{210}\text{Pb}$  has spin  $8^+$ . However, because the coupling constant  $\Lambda_1(28)$  [see Ref. 18, Eq. (6)] is small, the corresponding spectroscopic amplitude is also small [ $B(g_{9/2}, g_{7/2}; 8) = -0.005$ ].

In the case of even-parity single-particle states, this last process becomes relevant if we include in the calculation pairing phonons with odd angular momentum. A  $3^-$  level of  $^{210}\text{Pb}$  has recently been found to be rather low in excitation,<sup>19</sup> about 1.87 MeV. This state, coupled to a  $p_{1/2}$  hole, would lead to levels of spin and parity  $\frac{5}{2}^+$  and  $\frac{7}{2}^+$  which would lie about 4 MeV in excitation in  $^{209}\text{Pb}$  and could mix with the  $g_{7/2}$  and  $d_{5/2}$  single-particle states. However, both the inelastic scattering and the  $(t, p)$  cross sections indicate that the  $3^-$  state in  $^{210}\text{Pb}$  has an important component with both the particle-hole (03) phonon and the pairing (20) phonon present, in addition to the zero-order component (23) with only one boson. The cross-section ratios of this state to another possible  $3^-$  state at 2.85 MeV in  $^{210}\text{Pb}$  is 2:1, as seen in the  $(t, t')$  reaction. Moreover, a DW calculation of the  $(t, p)$  cross section associated with the 1.87-MeV state assuming pure  $(g_{9/2}, j_{15/2})$  configuration yields 0.20 of the experimental value. The inclusion of the  $(i_{11/2}, j_{15/2})$  configuration brings this value to 0.25. Therefore, in order to treat these effects within the framework of the model used in Paper I, the coupling between states in  $^{210}\text{Pb}$  having different numbers of phonons should be clarified first.

Probably, the transition to the  $\frac{7}{2}^+$  state would be more affected than the transition to the  $\frac{5}{2}^+$  state (the  $\frac{7}{2}^+$  lies higher in energy, the matrix element  $\langle p_{1/2} || Y_3 || g_{7/2} \rangle$  involves no spin flip as does the  $\langle p_{1/2} || Y_3 || d_{5/2} \rangle$ , etc.). Therefore, the discrepancy of Table III in the case of the  $g_{7/2}$  state could eventually be removed within the particle-vibrator model. However, we have not found any excuse for the  $s_{1/2}$  deviation. It should be

noted that the corresponding single-particle state extends far beyond the nuclear surface (this state has an extra node and no centrifugal barrier), and therefore, problems related to the self-consistency of the Woods-Saxon potential may become more important here (although the agreement for the one-body stripping suggests that these effects are small).

#### V. EXCITATION OF TWO-PARTICLE-ONE-HOLE STATES

The majority of the levels seen in the  $^{207}\text{Pb}(t, p)^{208}\text{Pb}$  reaction are of the two-particle-one-hole (2p-1h) type. As mentioned above, these may be reached by placing the two transferred particles into orbitals above the  $N=126$  shell while leaving the  $3p_{1/2}$  hole of the target nucleus empty. In their simplest form, such states are the coupling of the levels of  $^{210}\text{Pb}$ , which are the two-particle states, to this hole [ $(12\lambda; p_{1/2}; JM)$  states]. Experimentally, one can thus compare the  $^{208}\text{Pb}(t, p)^{210}\text{Pb}$  and the  $^{207}\text{Pb}(t, p)^{209}\text{Pb}$  spectra to obtain information on the structure of the levels observed in the latter reaction. This has been carried out in Ref. 6 for the lowest 2p-1h states and will be further pursued here. The  $^{210}\text{Pb}$  data are discussed in more detail elsewhere.<sup>20</sup>

A further check on the nature of the states observed in the  $(t, p)$  reaction is the information obtained in single-nucleon stripping<sup>3</sup> and pickup<sup>21</sup> reactions leading to  $^{209}\text{Pb}$ . The latter reaction is particularly useful because, in zero order, the 2p-1h levels excited in the  $^{210}\text{Pb}(p, d)^{209}\text{Pb}$  reaction are of the type [ $(120, i; JM)$ ]. In particular, the lowest of these will be for  $i=3p_{1/2}$ , thus being the same 2p-1h state excited by the  $(t, p)$  reaction. Additional levels with  $J^\pi \neq \frac{1}{2}^-$  may also be excited by both reactions but only if mixing between states of the same  $J^\pi$  occurs. If this is the case, the  $J^\pi$  value may be assigned uniquely by the formula<sup>9</sup>

$$J^\pi = \left( \frac{L+l}{2} \right)^{(-1)^l},$$

where  $L$  is the angular momentum transfer from the  $(t, p)$  reaction and  $l$  that of the  $(p, d)$  reaction.

Quite recently there has been additional information obtained on the stripping character of some of the 2p-1h states by means of the  $^{208}\text{Pb}(d, p)^{209}\text{Pb}$  reaction.<sup>22-24</sup> Such levels are only weakly populated in this reaction, and the interpretation of their observation is that  $^{208}\text{Pb}$  is not a completely closed shell but contains a certain amount of 2p-2h components. The presence of some 2p-2h components in the  $^{208}\text{Pb}$  ground state is in part a consequence of the zero-point motion associated with the vibrational spectrum.<sup>25</sup> Contributions to the

$^{208}\text{Pb}(d, p)^{209}\text{Pb}$  ( $2p-1h$ ) cross sections may also come from two-step processes such as inelastic scattering to an excited state of  $^{208}\text{Pb}$  and then stripping to the observed level. The quantitative importance of two-step processes awaits theoretical assessment.

In addition to these simple experimental comparisons, a comparison can also be made with the theoretical calculations given in Paper I. These calculations include the possibility of mixing the states of the same spin and parity which would be directly excited by the  $(t, p)$  or  $(p, d)$  reactions. The obvious states to be included are the multiplets<sup>17</sup> based on collective states of  $^{208}\text{Pb}$  coupled to the  $g_{9/2}$  particle, i.e., states of the type  $|103, g_{9/2}; JM\rangle$  and the multiplets based on the low-lying states of  $^{210}\text{Pb}$  coupled to the hole states of  $^{207}\text{Pb}$ , i.e., states of the type  $|121, i; JM\rangle$ . The full description of the technique and parameters used in the calculation are given in Paper I.

#### A. $J^\pi = \frac{1}{2}^-$ States

Only one  $L=0$  transition was seen in the  $^{207}\text{Pb}(t, p)^{209}\text{Pb}$  reaction. This state is at 2.152 MeV and its angular distribution is shown in Fig. 4 where it is compared to the ground-state transition of the  $^{208}\text{Pb}(t, p)^{210}\text{Pb}$  reaction. The DW calculations for these levels are also shown in this figure; the search for the parameters to fit this  $L=0$  transition is discussed above. The observed two-neu-

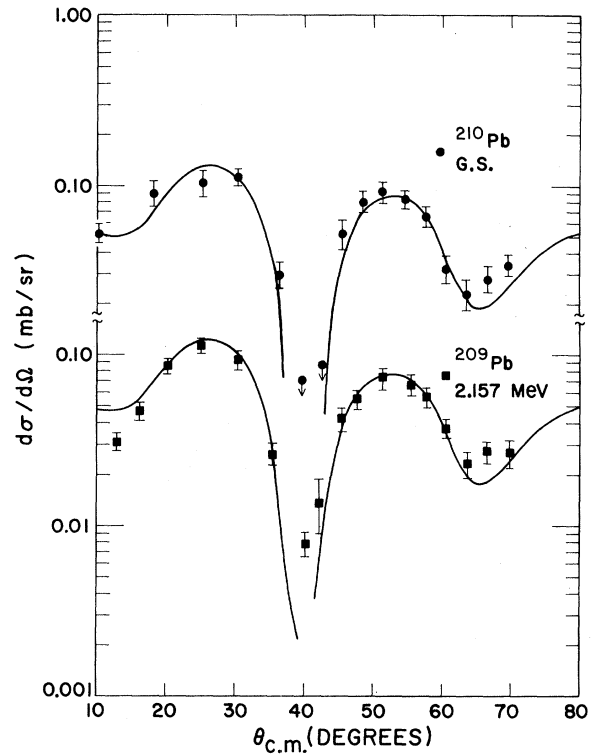


FIG. 4.  $L=0$  transitions as seen in  $^{209}\text{Pb}$  and the lowest such transition in  $^{210}\text{Pb}$ . The solid line is the result of a DW calculation.

TABLE IV. Experimental comparison of  $^{207}\text{Pb}(t, p)^{209}\text{Pb}$  and  $^{208}\text{Pb}(t, p)^{210}\text{Pb}$  cross sections.

$E_x(^{209}\text{Pb})$ (MeV)	$L$	$J^\pi$	$\frac{\sigma(209)}{\sigma(210)}$	$\sum \frac{\sigma(209)}{\sigma(210)}$	Centroid relative to 2152-MeV level (MeV)	$E_x(^{210}\text{Pb})$ (MeV)
2.152	0	$\frac{1}{2}^-$	1.02	1.02	0	0
2.737	2	$\frac{5}{2}^-$	0.25	1.02	0.697	0.795
2.868	2	$\frac{5}{2}^-$	0.38			
2.902	2	$\frac{3}{2}^-$	0.38			
3.028	4	$\frac{7}{2}^-$	0.56	1.06	0.955	1.092
3.206	4	$\frac{9}{2}^-$	0.45			
3.072	6	$(\frac{11}{2}^-)$	0.43	1.00	1.056	1.187
3.309	6	$(\frac{13}{2}^-)$	0.58			
3.100	(8)	$(\frac{15}{2}^-, \frac{17}{2}^-)$	0.41	1.07	1.198	1.268
3.432	8	$(\frac{15}{2}^-, \frac{17}{2}^-)$	0.30			
3.561	8	$(\frac{15}{2}^-, \frac{17}{2}^-)$	0.36			
3.708	(3)	$(\frac{5}{2}^+, \frac{7}{2}^+)$	0.28	0.68	1.786	1.870
4.100	(3)	$(\frac{5}{2}^+, \frac{7}{2}^+)$	0.40			

tron separation energy for this level is only 40 keV lower than that for the ground state of  $^{210}\text{Pb}$  and the cross sections for both transitions are equal to within the experimental errors as can be seen by Table IV. This is in agreement with the  $^{210}\text{Pb}(p, d)^{209}\text{Pb}$  observation of all of the  $p_{1/2}$  strength being located at this energy.<sup>21</sup>

The results of the calculations of Paper I are shown in Table V. Neither experiment nor theory indicate that levels other than the one having as main component the  $|120; p_{1/2}; \frac{5}{2}M\rangle$  states populated in both the two-body stripping and the one-body pickup reactions (see Table VI). Therefore, this agreement between theory and experiment is not significant evidence favoring the model of Paper I, since the zero-order approximation (see Fig. 10) yields the same result.

#### B. $J^\pi = \frac{3}{2}^-, \frac{5}{2}^-$ States

A number of levels populated with  $L = 2$  ( $t, p$ ) are seen in the spectrum as is indicated in Fig. 5. We divide the following discussion in two main parts, one in which the experimental  $^{207}\text{Pb}(t, p; L = 2)^{209}\text{Pb}$  data are presented, and in which the help of the  $^{210}\text{Pb}(p, d)$  reaction and the zero-order coupling model is used to assign configurations. In a second part, the predictions of model I are discussed.

The lowest, more intense transitions are expected to populate the  $|122; p_{1/2}; JM\rangle$  states with  $J = \frac{3}{2}, \frac{5}{2}$ . However, four states are seen in the energy region where this strength is anticipated, these being at 2.737, 2.868, 2.902 MeV, and a rather weak state at 2.992 MeV. In the 13-MeV  $^{207}\text{Pb}(t, p)^{209}\text{Pb}$  experiment of Bjerregaard *et al.*,<sup>7</sup> it was suggested that the  $\frac{5}{2}^-$  strength at 2.873 MeV had mixed with a nearby  $\frac{5}{2}^-$  level at 2.737 MeV which would correspond mainly to the  $|120; f_{5/2}; \frac{5}{2}M\rangle$  configuration. The  $^{210}\text{Pb}(p, d)^{209}\text{Pb}$  results confirm this hypothesis from the  $l = 3$  assignment and the large spectroscopic factor for an assumed  $2f_{5/2}$  pickup.<sup>6, 21</sup>

The level at 2.902 MeV is confirmed to be a  $\frac{3}{2}^-$  state by the  $l = 1$  angular distribution of the pickup reaction. The largest pickup spectroscopic factor with  $l = 1$  is associated with a level at 3.077 MeV. Therefore, in zero order we ascribe the configurations  $(122; p_{1/2}; \frac{3}{2}M)$  and  $(120; p_{3/2}; \frac{3}{2}M)$  to the levels at 2.902 and 3.072 MeV, respectively. [The latter level is presumably not the 3.077 level seen in the ( $t, p$ ) results; see below.]

The theoretical calculations of Paper I are presented and compared to the data in Table VI. The observed splitting between the  $(122; p_{1/2}; JM)$  states (0.133 MeV) is not reproduced although some splitting is predicted. The predicted excitation energies are approximately correct for

the three levels and in the correct order.

The three stronger levels account for all of the ( $t, p$ ) strength seen to the lowest  $2^+$  of  $^{210}\text{Pb}$  and their centroid is in agreement with the excitation energy of this state as can be seen from Table IV. Theoretically, this is true in zero order and in the calculation done in Paper I (see Fig. 10). In the case of the pickup reactions, most of the reaction strength is also concentrated at a definite energy (see Table V). This energy agrees reasonably well with the experimental number, but again this is true in the zero-order approximation. However, the spectroscopic factors for the ( $p, d$ ) reaction agree with the theoretical predictions only after the diagonalization has been made (see Table V of Paper I). As mentioned previously, the model

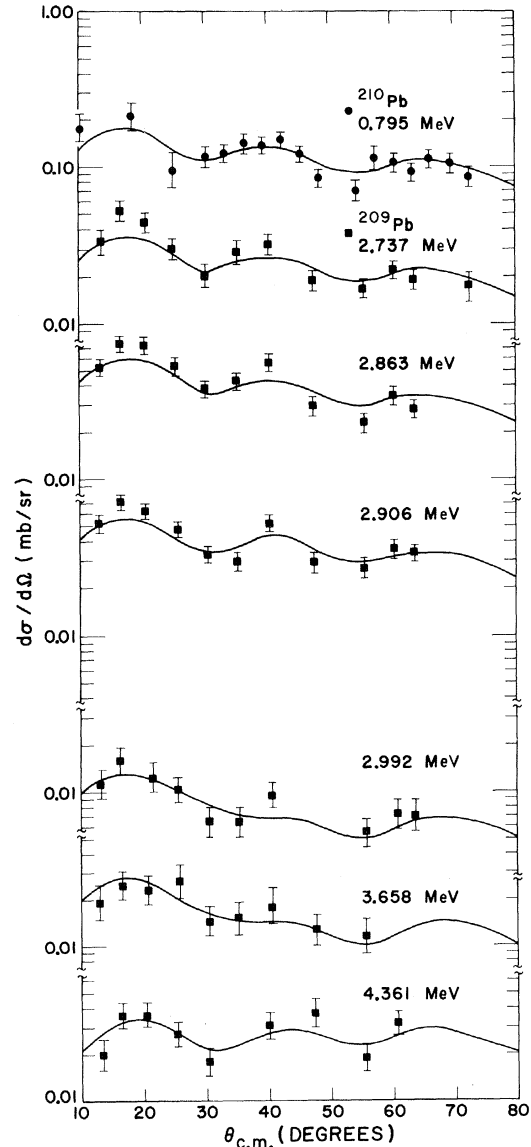


FIG. 5.  $L = 2$  transitions; see Fig. 4 caption.

TABLE V. The excitation energies given are those predicted in Ref. 17. Also noted are the relevant configurations from these calculations, and the spectroscopic factors predicted and obtained from the  $^{210}\text{Pb}(p,d)^{209}\text{Pb}$  reaction of Ref. 21. [ $\Sigma$  indicates the calculated pickup sum-rule limits as discussed in Paper I, Eq. (32).]

(a) $J^\pi = \frac{1}{2}^-$															
Theory ( $\Sigma = 1.83$ )															
$E(\text{MeV})$	2.22	3.57	3.82												
S	1.83	0.00	0.00												
$a(120; p_{1/2}; \frac{1}{2})$	1.00	0.03	0.01												
(b) $J^\pi = \frac{3}{2}^-$															
Theory ( $\Sigma = 3.71$ )															
$E(\text{MeV})$	2.36	2.98	3.19	3.55	3.79										
S	1.21	0.20	2.60	0.00	0.01										
$a(122; p_{1/2}; \frac{3}{2})$	-0.11	0.97	0.20	0.03	-0.02										
$a(222; p_{1/2}; \frac{3}{2})$	-0.03	0.01	0.03	0.02	0.02										
$a(322; p_{1/2}; \frac{3}{2})$	-0.05	0.02	0.04	0.02	0.02										
$a(103; g_{9/2}; \frac{3}{2})$	0.91	0.03	0.29	0.09	-0.04										
$a(120; p_{3/2}; \frac{3}{2})$	0.32	0.23	-0.91	-0.08	0.04										
Experiment															
$E(\text{MeV})$	2.320	2.906	3.031	3.077	3.524	3.562	3.627								
S	0.50	0.20	0.01	2.62	0.03	0.02	0.11								
(c) $J^\pi = \frac{5}{2}^-$															
Theory ( $\Sigma = 5.62$ )															
$E(\text{MeV})$	2.37	2.79	2.98	3.40	3.60										
S	0.51	5.21	0.08	0.01	0.01										
$a(122; p_{1/2}; \frac{5}{2})$	-0.04	-0.14	0.99	-0.02	-0.03										
$a(222; p_{1/2}; \frac{5}{2})$	-0.01	-0.01	-0.01	0.02	0.02										
$a(322; p_{1/2}; \frac{5}{2})$	-0.02	-0.01	-0.01	0.02	0.03										
$a(103; g_{9/2}; \frac{5}{2})$	-0.96	-0.19	-0.07	-0.02	-0.02										
$a(120; f_{5/2}; \frac{5}{2})$	-0.20	-0.96	0.12	-0.11	-0.08										
Experiment															
$E(\text{MeV})$	2.463	2.741	2.873												
S	0.61	4.76	1.02												
(d) $J^\pi = \frac{7}{2}^-$															
Theory ( $\Sigma = 7.75$ )															
$E(\text{MeV})$	2.61	3.22	3.34	3.56	3.79	3.85	3.89	4.10	4.11	4.24	4.51	4.56	4.63		
S	0.13	0.00	0.01	0.00	0.00	0.00	0.01	0.00	0.00	0.06	0.66	5.15	0.05		
$a(124; p_{1/2}; \frac{7}{2})$	-0.07	-1.00	0.05	0.01	-0.01	0.00	0.01	0.00	0.00	-0.02	0.00	0.01	0.00		
$a(224; p_{1/2}; \frac{7}{2})$	-0.03	0.01	-0.01	0.00	0.01	0.00	-0.02	0.72	-0.67	-0.15	0.00	0.02	-0.01		
$a(324; p_{1/2}; \frac{7}{2})$	-0.04	0.01	-0.01	0.00	0.01	0.00	-0.01	0.02	0.01	0.15	0.92	0.24	-0.08		
$a(103; g_{9/2}; \frac{7}{2})$	0.97	-0.06	0.10	-0.02	-0.01	0.03	0.09	0.05	0.03	-0.05	0.02	0.05	0.02		
$a(120; f_{7/2}; \frac{7}{2})$	0.05	-0.01	0.02	0.01	-0.01	0.01	0.04	0.02	0.00	-0.08	0.33	-0.92	-0.09		
Experiment															
$E(\text{MeV})$	2.563	3.028	3.499	3.906	4.212	4.222	4.270	4.309	4.395	4.562	4.584	4.671	4.690	4.714	4.781
S	0.02	0.16	0.11	0.91	2.08	1.44	0.91	0.06	0.32	0.14	0.09	0.25	0.17	0.11	

TABLE V (Continued)

(e) $J^\pi = \frac{9}{2}^-$						(j) $J^\pi = \frac{1}{2}^+$					
Theory ( $\Sigma = 9.84$ )						Theory					
$E(\text{MeV})$	2.47	3.21	3.41	3.56	3.79	$E(\text{MeV})$	4.98		5.79		
S	0.00	0.00	0.02	0.00	0.00	S	0.00		0.00		
$a(124; p_{1/2}; \frac{9}{2})$	0.04	-0.99	-0.11	0.03	0.00						
$a(224; p_{1/2}; \frac{9}{2})$	0.02	0.00	0.03	-0.02	-0.01	(k) $J^\pi = \frac{3}{2}^+$					
$a(324; p_{1/2}; \frac{9}{2})$	0.03	0.00	0.04	-0.02	-0.01	Theory					
$a(103; g_{9/2}; \frac{9}{2})$	0.99	0.04	0.01	-0.04	-0.02	$E(\text{MeV})$	4.94		5.74		
$a(120; g_{9/2}; \frac{9}{2})$	0.00	0.00	0.02	-0.01	-0.01	S	0.00		0.00		
Experiment						(l) $J^\pi = \frac{5}{2}^+$					
$E(\text{MeV})$				3.206		Theory					
S						$E(\text{MeV})$	4.94		4.87		
(f) $J^\pi = \frac{11}{2}^-$						S					
Theory ( $\Sigma = 11.94$ )						0.00					
$E(\text{MeV})$	2.68	3.28	3.32	3.79		(m) $J^\pi = \frac{7}{2}^+$					
S	0.00	0.00	0.00	0.00		Theory					
$a(126; p_{1/2}; \frac{11}{2})$	-0.08	-0.98	0.18	0.00		$E(\text{MeV})$	4.86	4.93	4.97		
$a(226; p_{1/2}; \frac{11}{2})$	-0.05	0.00	-0.01	0.00		S	0.00	0.00	0.00		
$a(103; g_{9/2}; \frac{11}{2})$	0.98	-0.06	0.10	0.00		(n) $J^\pi = \frac{9}{2}^+$					
$a(120; i_{11/2}; \frac{11}{2})$	0.00	0.00	0.00	0.00		Theory					
(g) $J^\pi = \frac{13}{2}^-$						S					
Theory						4.21 4.64 4.93 4.86 5.73					
$E(\text{MeV})$	2.51	3.27	3.44	3.79		$E(\text{MeV})$	4.02	4.61	4.86	4.93	5.73
S	0.00	0.00	0.00	0.00		S	0.00	0.00	0.00	0.00	0.00
$a(126; p_{1/2}; \frac{13}{2})$	0.03	-0.97	-0.23	-0.01		$a(103; j_{15/2}; \frac{9}{2})$	0.01	0.00	0.00	0.00	0.00
$a(226; p_{1/2}; \frac{13}{2})$	0.02	-0.02	0.08	0.01		(o) $J^\pi = \frac{11}{2}^+$					
$a(103; g_{9/2}; \frac{13}{2})$	1.00	0.02	0.05	0.02		Theory					
(h) $J^\pi = \frac{15}{2}^-$						S					
Theory						4.02 4.61 4.86 4.93 5.73					
$E(\text{MeV})$	3.22	3.32	3.47	3.85		$E(\text{MeV})$	3.83	4.11	4.62	4.86	4.92
S	0.06	0.00	0.09	0.00		S	12.59	0.16	0.01	0.00	0.00
$a(128; p_{1/2}; \frac{15}{2})$	0.07	0.99	0.14	-0.01		$a(120; i_{13/2}; \frac{13}{2})$					
$a(103; g_{9/2}; \frac{15}{2})$	0.70	0.06	-0.71	0.03		$a(103; j_{15/2}; \frac{13}{2})$					
$a(103; i_{11/2}; \frac{15}{2})$	0.71	-0.15	0.69	0.01		(p) $J^\pi = \frac{13}{2}^+$					
(i) $J^\pi = \frac{17}{2}^-$						Theory ( $\Sigma = 13.74$ )					
Theory						S					
$E(\text{MeV})$	3.30	3.58	3.85	3.89		$E(\text{MeV})$	3.659	3.751	3.811	3.937	3.995
S	0.00	0.00	0.00	0.00		S	11.80	0.14	0.32	0.92	0.41
$a(128; p_{1/2}; \frac{17}{2})$	0.98	0.18	-0.01	-0.01		Experiment					
$a(103; i_{11/2}; \frac{17}{2})$	0.18	-0.96	0.12	0.16		$E(\text{MeV})$	3.659	3.751	3.811	3.937	3.995
						S	11.80	0.14	0.32	0.92	0.41

is effectively tested by the predicted mixing of unperturbed levels and the consequent fractioning of the different cross sections. In the case of  $\frac{3}{2}^-$  states, both experiment and theory agree that the  $(t, p)$  cross section goes mainly to a single state. Theoretically, however, there is a weak component which is expected to populate the  $(120; p_{3/2}, \frac{3}{2}M)$  state at 3.072. This level was identified in the  $^{210}\text{Pb}(p, d)$  reaction. Experimentally, there is a weak component populating a level at 2.992 MeV, but it is difficult to reconcile experimentally these two energies.

Both theory and experiment agree with a pickup spectroscopic factor of 0.20 for the population of the  $(122; p_{1/2}, \frac{3}{2}M)$  state at 2.152 MeV. In the  $\frac{5}{2}^-$

case, there are two states seen in the  $(t, p)$  reaction whereas the model predicts only one at 2.98 MeV. The  $(p, d)$  spectroscopic factor of the state at 2.87 MeV is an order of magnitude larger than the predicted one [see Table V(c)]. Therefore, the predicted mixing between the two  $\frac{3}{2}^-$  states is well reproduced, while it is too small in the case of  $\frac{5}{2}^-$  states. A discussion is given in Paper I concerning this small mixing. It is very significant from the theoretical point of view, because it will probably require the introduction of terms with two phonons in the coupling Hamiltonian in order to simulate those effects of the usual quad-

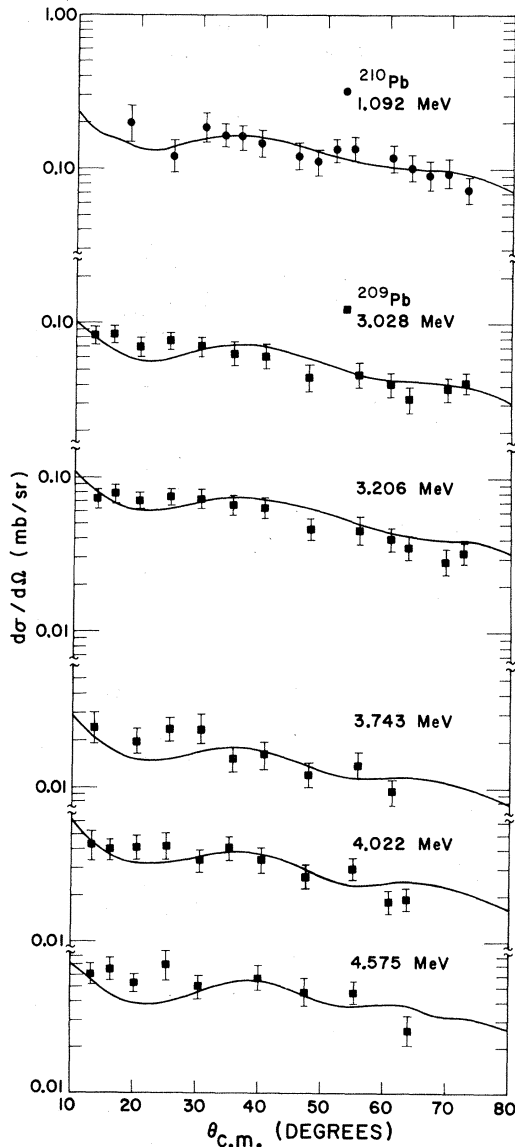


FIG. 6.  $L=4$  transitions; see Fig. 4 caption.

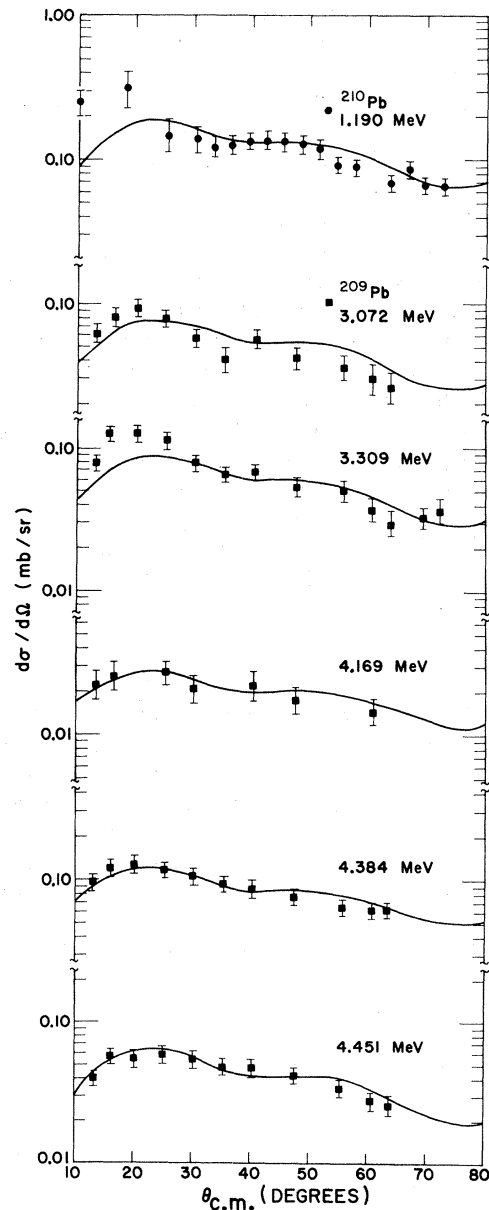


FIG. 7.  $L=6$  transitions; see Fig. 4 caption.

rupole force which are discussed in Paper I.

C.  $J^\pi = \frac{7}{2}^-, \frac{9}{2}^-$  States

The lowest ( $L = 4$ ) state in  $^{210}\text{Pb}$  is located at 1.092 MeV<sup>6</sup> and is apparently split into only two observable components in  $^{209}\text{Pb}$ . The transitions leading to states at 3.028 and 3.206 MeV appear to have an  $L = 4$  character when compared to the  $L = 4$  of  $^{210}\text{Pb}$  in Fig. 6 and also are reasonably described by the DW calculation. The centroid of these two levels is also in approximate agreement with the excitation energy of the (1.092 MeV) state in  $^{210}\text{Pb}$  and the summed cross section is also correct as indicated in Table IV. The theoretical cross sections of Paper I are in agreement with these states as is shown in Table VI. The observed energy splitting is, however, greater than predicted in Tables V(d) and V(e) (see also Table VI), 178 keV versus only 8 keV, which is similar to the disagreement found for the splitting of the  $(122; p_{1/2}; JM)$  states. The lower member of this doublet would appear to be the  $\frac{7}{2}^-$  member based on the fact that it is seen in the  $^{210}\text{Pb}(p, d)-^{209}\text{Pb}$  experiment as an  $l = 3$  transfer. Additional possible  $L = 4$  states are seen at higher excitation and presumably have their parentage in higher excited  $4^+$  states of  $^{210}\text{Pb}$ . Possible candidates for these levels are the (see Table VI) 3.743 MeV, a  $\frac{9}{2}^-$  level, 4.022 MeV, a  $\frac{9}{2}^-$  level, and 4.578 MeV, a  $\frac{7}{2}^-$  level. The intensities predicted for such states are all in reasonable agreement with the experimental values. The state predicted to be at 4.511 MeV should have a cross section twice that of the lowest  $L = 4$  transfer.

D.  $J^\pi = \frac{11}{2}^-, \frac{13}{2}^-$  States

As in the case of the  $(t, p)$   $L = 4$  transfers, only two  $L = 6$  cases appear to be in the region of excitation expected for the  $(126; p_{1/2}; JM)$  states with  $J^\pi = \frac{11}{2}^-, \frac{13}{2}^-$ . These are at 3.072 and 3.309 MeV and are shown in Fig. 7 where they are compared to the lowest  $6^+$  state of  $^{210}\text{Pb}$  at 1.187 MeV. Again Table IV indicates reasonable agreement between the energy centroid of the  $L = 6$  levels of  $^{209}\text{Pb}$  and the  $6^+$  state of  $^{210}\text{Pb}$ . Also the sum of the cross sections for the two  $^{209}\text{Pb}$  levels is in agreement with the measured cross section of the  $^{210}\text{Pb}$   $6^+$  state as seen in this table. The theoretical predictions for these levels are given in Table V, and the comparisons to the present data are shown in Fig. 7. The corresponding DW calculations are shown in Fig. 7. Again the observed splitting of 237 keV is much larger than the predicted value of 12 keV. Several states at higher excitations are also possible  $L = 6$  candidates as seen in Fig. 7. The levels at 4.169, 4.384, and 4.451 MeV fit

this description and when compared to the theoretical estimates of strengths at these excitations in Table VI, reasonable agreement, to within 40%, is obtained. Several of these higher  $L = 6$  transfers are a factor of 2.5 larger in cross section than the lowest  $6^+$  states for the  $(t, p)$  reaction, and this is predicted by the model of Paper I. Pickup is not expected to be observed to  $\frac{11}{2}^-$  and  $\frac{13}{2}^-$  states, as there are no single-particle states of those spins and parities in the two shells which are closest to the Fermi surface. (The  $h_{11/2}$  single-particle orbit is approximately 9 MeV below the Fermi surface.)

E.  $J^\pi = \frac{15}{2}^-, \frac{17}{2}^-$  States

Three  $(t, p)$  transitions of possible  $L = 8$  character are identified in Table IV populating states at 3.100, 3.432, and 3.561 MeV. These are com-

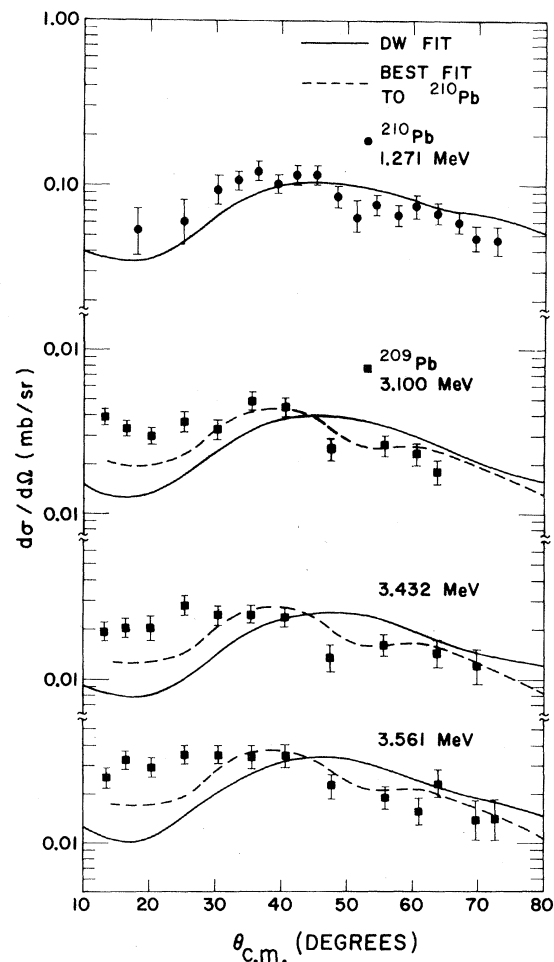


FIG. 8.  $L = 8$  transitions; see Fig. 4 caption. Also, the dashed line is a smooth curve drawn through the  $^{210}\text{Pb}$  data to better ascertain the  $L = 8$  character of these states in  $^{209}\text{Pb}$ .

pared to the transition to the  $8^+$  state of  $^{210}\text{Pb}$  in Fig. 8 and also to DW calculations using the two-nucleon spectroscopic amplitudes of Paper I. The rather featureless angular distributions and the poor fit to DW theory leave their assignment somewhat ambiguous, but the comparison to the  $8^+$  of  $^{210}\text{Pb}$  is still meaningful and this is emphasized in Fig. 8. Experimentally, these three states in  $^{209}\text{Pb}$  are required to obtain the full strength seen in  $^{208}\text{Pb}$ , as shown in Table IV, with their sum giving an acceptable ratio to  $^{210}\text{Pb}$  and their energy centroid in good agreement with the position of the 1.268-MeV  $8^+$  state of  $^{208}\text{Pb}$ .

It had been suggested in Ref. 6 that a possible reason for three such states lies in the fractionation of the  $\frac{15}{2}^-$  levels. The  $^{208}\text{Pb}(t, d)^{209}\text{Pb}$  reaction<sup>3</sup> indicates that the  $1j_{15/2}$  single-particle state is indeed not pure. (It is probably mixed with the  $|103; g_{9/2}, \frac{15}{2}\rangle$  state.) The additional single-particle strength would then lie higher in excitation but should be seen in single-particle and two-

particle transfer reactions. Ellegaard, Kantele, and Vedelsby<sup>23</sup> have proposed a tentative assignment of a level at 3.310 MeV as a  $\frac{15}{2}^-$  level. The present analysis, however, suggests the level, seen here at 3.309 MeV, is a  $\frac{13}{2}^-$  or  $\frac{11}{2}^-$  state. A level seen in the work of Ellegaard, Kantele, and Vedelsby<sup>23</sup> at 3.556 MeV could very well correspond to the 3.561-MeV state suggested above and be at least part of the missing  $\frac{15}{2}^-$  strength. This would explain the splitting of the  $|128; p_{1/2}, \frac{15}{2} M\rangle$  components of the doublet. Presumably the  $\frac{17}{2}^-$  member is largely unperturbed.

Because the matrix element

$$\langle j_{15/2} | h(03) | 103; g_{9/2}, \frac{15}{2} \rangle$$

is very large, it is possible to excite  $\frac{15}{2}^-$  states in the  $^{210}\text{Pb}(p, d)$  reaction through processes represented by graphs (c) and (d) of Fig. 8 of Paper I, where  $k=j_{15/2}$ ,  $k=g_{9/2}$ , and  $\lambda_2^\pi = 3^-$ . The  $J^\pi = \frac{15}{2}^-$  state carrying the largest predicted  $l=7$  pickup intensity is the state at 3.47 MeV [see Table V(h)].

TABLE VI. Comparison of experimental and theoretical (see Ref. 17) cross sections and energy positions of levels excited in the  $^{207}\text{Pb}(t, p)^{208}\text{Pb}$  reaction.

Excitation energy (MeV)		$L$	$J^\pi$	$\sigma(\text{exp})/\sigma(\text{theo})^a$	
Experimental	Theoretical			Unnormal	Norm. <sup>b</sup>
2.152	2.223	0	$\frac{1}{2}^-$	0.58	1.00
2.737	2.786	2	$\frac{5}{2}^-$	3.54	6.10
2.868	2.983	2	$\frac{5}{2}^-$	0.30	0.52
2.902	2.979	2	$\frac{3}{2}^-$	0.39	0.68
3.028	3.220	4	$\frac{7}{2}^-$	0.55	0.95
3.072	3.282	6	$(\frac{11}{2}^-)$	0.48	0.83
3.100	3.301	8	$(\frac{17}{2}^-)$	0.48	0.83
3.206	3.212	4	$\frac{9}{2}^-$	0.34	0.60
3.309	3.270	6	$(\frac{13}{2}^-)$	0.55	0.95
3.432	3.323	8	$(\frac{15}{2}^-)$	0.39	0.67
3.561	3.472	8	$(\frac{15}{2}^-)$	30.0	52.0
3.659	4.102	(2)	$(\frac{3}{2}^-)$	0.61	1.06
3.743	4.110	(4)	$(\frac{9}{2}^-)$	0.41	0.71
4.169	4.083	(6)	$(\frac{13}{2}^-)$	0.20	0.35
4.361	4.310	(2)	$(\frac{3}{2}^-)$	0.47	0.81
4.384	4.070	(6)	$(\frac{11}{2}^-)$	0.88	1.52
4.451		(6)	$(\frac{13}{2}^-)$		
4.022	4.509	(4)	$(\frac{11}{2}^-)$	0.52	0.89
4.578	4.511	(4)	$(\frac{7}{2}^-)$	0.22	0.38
4.632	4.688	(6)	$(\frac{11}{2}^-)$	0.52	0.89

<sup>a</sup> $\sigma(\text{theo})$  obtained from normalization of 310 using Ref. 18.

<sup>b</sup>The 2.152-MeV state ratio is set equal to one. The purpose of the normalized column is to indicate the ratios of the  $\sigma(\text{exp})/\sigma(\text{theo})$  for the various states.

Experimentally, the state at 3.561 MeV is a possible candidate for this assignment.

The model of Paper I does not produce a sufficient mixing between the predicted  $\frac{15}{2}^-$  states at 3.22, 3.32, and 3.47 MeV in order to explain the  $(t, p)$  results.

#### F. $J^\pi = \frac{1}{2}^+, \frac{3}{2}^+$ States

Within our basic subset of states the only available configurations for these states are  $(12\lambda; i_{13/2}; JM)$  with  $\lambda = 6, 8$  (see Table V). None of the employed reactions can excite these configurations in a significant way.

#### G. $J^\pi = \frac{5}{2}^+, \frac{7}{2}^+$ States

Two  $L = 3$  transfers should be seen in going to states in  $^{209}\text{Pb}$  which may be represented as a  $p_{1/2}$  hole coupled to the  $3^-$  state of  $^{210}\text{Pb}$  at 1.8 MeV. Two states have been identified as possible  $L = 3$  transfers. These are at 3.708 MeV with a ratio of 0.28 of the  $|^{210}\text{Pb}(3^-)\rangle$  and at 4.100 MeV with a ratio of 0.40 of this same state (see also Table IV and Fig. 9). The centroid of these levels is at 3.939 MeV which is approximately the correct excitation energy relative to the 2.152-MeV state or at 4.022 MeV, and with about 70% of the total expected strength observed. The  $2J+1$  rule would suggest the lower member has  $\frac{5}{2}^+$  and

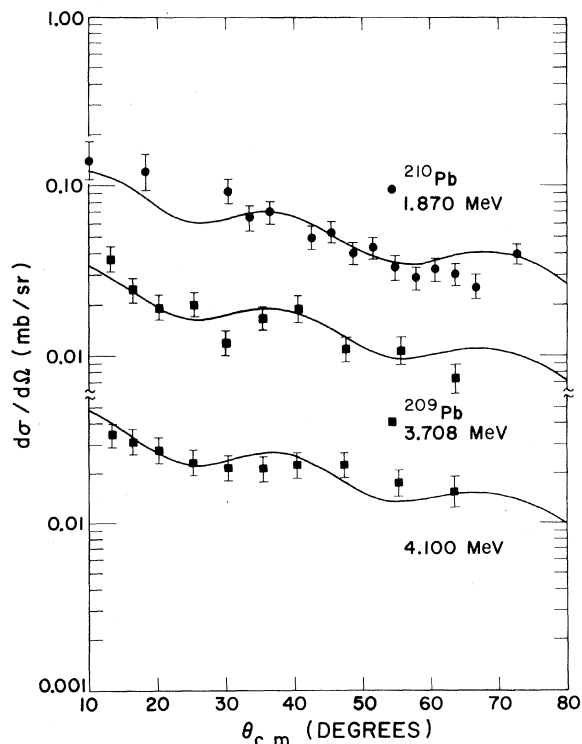


FIG. 9.  $L = 3$  transitions; see Fig. 4 caption.

the upper is of  $\frac{7}{2}^+$  spin but since all of the strength is not observed this is rather indefinite. Should such states be mixed with the lower single-particle states they should be observed in single-particle stripping experiments through the latter components. In the  $^{208}\text{Pb}(d, p)^{209}\text{Pb}$  experiment of Ellegaard, Kantele, and Vedelsby<sup>23</sup> no states were seen in the region of 3.7 MeV, but levels at 4.095 and 4.113 MeV were seen, and one of these could correspond to the state observed here at 4.100 MeV. No spin assignments were made to these levels in the work of Ref. 22. The observation of the higher state would be in accord with a possible  $\frac{7}{2}^+$  assignment since such a state would mix stronger with the  $2g_{7/2}$  particle state than for the case of the  $\frac{5}{2}^+$  levels because of the nearer proximity of the  $2g_{7/2}$  level to the states in question.

It was noted in Sec. IV that the properties of the  $3^-$  state in  $^{210}\text{Pb}$  cannot be accounted for unless there is a considerable mixing of states having a different number of phonons. Consequently, the basic subset of states used in Paper I (consisting of a particle or a hole coupled to a single phonon) cannot explain the intensities of the  $L = 3$  transitions [see Tables V(1) and V(m)].

#### H. $J^\pi = \frac{9}{2}^+, \frac{11}{2}^+$ States

No definite  $(t, p)$   $L = 5$  transfers could be assigned. No  $5^-$  assignment has been made for  $^{210}\text{Pb}$  so it is difficult to establish where the  $L = 5$  strength would be in  $^{209}\text{Pb}$ . Such states would have spin and parity of  $\frac{9}{2}^+$  and  $\frac{11}{2}^+$  and could mix with the low-lying  $2g_{9/2}$  and  $i_{11/2}$  single-particle states. The same discussion given for the  $\frac{5}{2}^+$  and  $\frac{7}{2}^+$  levels probably applies here, although there is less evidence on the corresponding states in  $^{210}\text{Pb}$ . See also Tables V(n) and V(o).

#### I. $J^\pi = \frac{13}{2}^+$ States

These states have a component which is relevant for the pickup reaction, namely the  $(120; i_{13/2}; \frac{13}{2}M)$  configuration. Experimentally, the pickup intensity is somewhat more fractionated than it is theoretically [see Table V(n)].

## VI. DISCUSSION OF RESULTS

The  $^{207}\text{Pb}(t, p)^{209}\text{Pb}$  reaction excites a large number of states in the residual nucleus. It appears that by a rather simple comparison to results of a variety of other experiments such as single-nucleon pickup and stripping that the parentage of a number of the states can be interpreted. Moreover, the theoretical treatment given in Paper I using multipole pairing and particle-hole fields also gives a reasonable qualitative picture of the

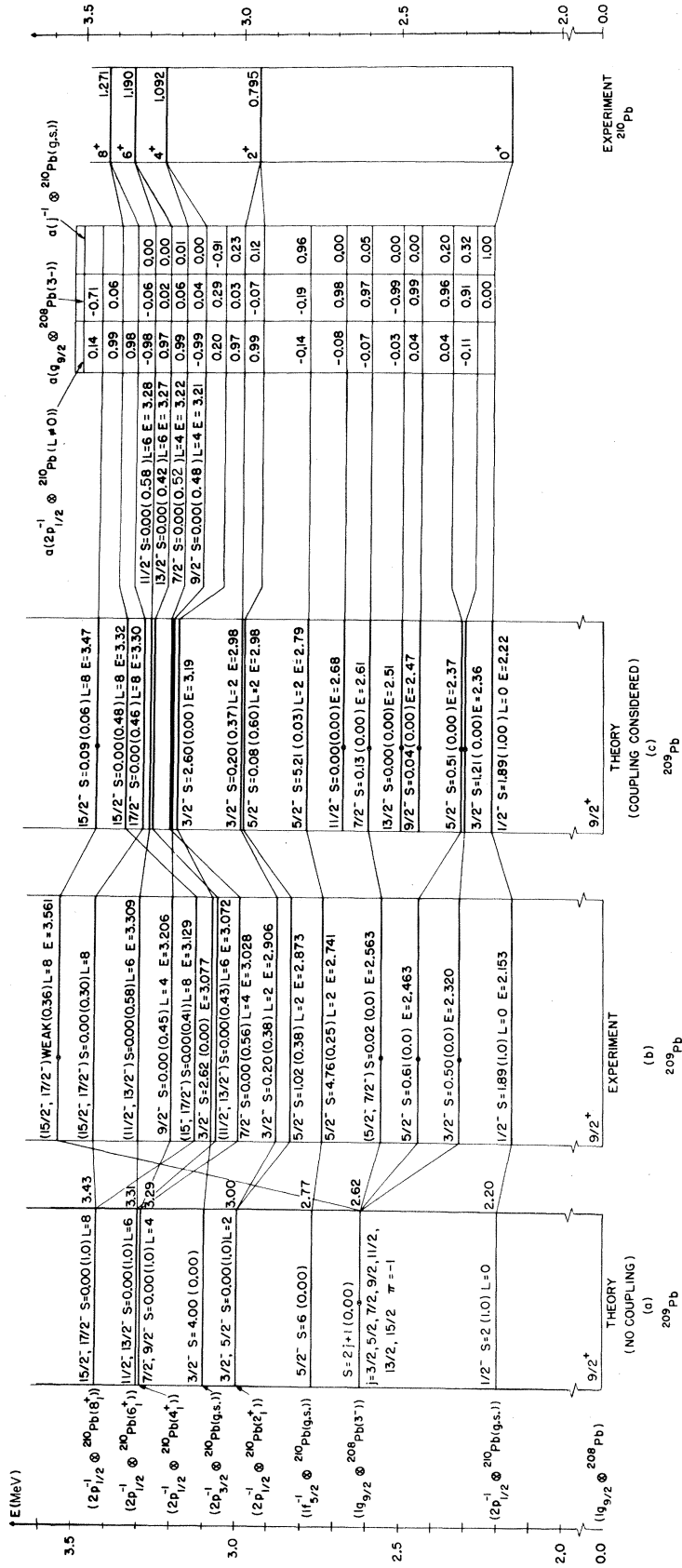


FIG. 10. Comparison of energy levels seen experimentally and as predicted by the calculations of Ref. 17.

states below 5 MeV in excitation energy. Above this energy there still exists a large number of levels excited in this reaction but the complexity of the spectrum becomes too difficult to interpret.

Figure 10 summarizes the comparison of experimental and theoretical results. The indication is that the position of the various doublets is reproduced to within 200 keV, which is quite rewarding. The principal discrepancies lie in the small amount of splitting calculated (about 10 keV for each doublet, as compared to the observed splitting of 100 to 200 keV) and also in the failure of the model to predict the  $\frac{5}{2}^-$  and  $\frac{15}{2}^-$  mixing observed experimentally.

It is interesting to point out the possible members of the  $[2g_{9/2}]^{208}\text{Pb}(3)_j$  multiplet using the experimental results obtained here and in Ref. 21. Tentative assignment for these members is shown in Fig. 10 as a splitting of the  $^{208}\text{Pb}(3)$  at 2.62 MeV. The figure suggests that the  $\frac{3}{2}^-$  member is at 2.320 MeV, the  $\frac{5}{2}^-$  member at 2.463 MeV, the  $\frac{7}{2}^-$  members possibly at 2.563 MeV, and the  $\frac{15}{2}^-$  member at 3.561 MeV. This latter assignment would be in agreement with the recent  $l=7$  assignment given in Ref. 23 to this state. The  $\frac{9}{2}^-$ ,  $\frac{11}{2}^-$ , and  $\frac{13}{2}^-$  members are less clear because there seems to be little mixing with configurations directly excited by

either the  $^{207}\text{Pb}(t,p)^{208}\text{Pb}$  or the  $^{210}\text{Pb}(p,d)^{208}\text{Pb}$  reactions, although the former certainly excites states of the correct spin and parity.

One of the results of the present experiment has been the use of the single-particle states to obtain an empirical absolute normalization factor for the two-particle transfer DW code of Bayman and Kallio. Such a result has already been used as a foundation in showing that, at least for a systematic analysis, a useful normalization over a wide range of mass can be obtained.<sup>18</sup> Moreover, within experimental errors, the same normalization is obtained for data at 13 and at 20 MeV, implying a quite reasonable energy range of usefulness. The DW treatment also gives a reasonably good explanation of the distributions observed experimentally, these being based on optical-model parameters which describe the single  $L=0$  transition observed.

#### VII. ACKNOWLEDGMENTS

The authors wish to thank S. Orbesen for his assistance in obtaining the data for this experiment, and also the Los Alamos and Yale scanning groups—in particular, Rexine Booth—for the excellent scanning of the spectrograph plates.

\*Work performed under the auspices of the U. S. Atomic Energy Commission.

†Presently at Carnegie-Mellon University, Pittsburgh, Pennsylvania 15213.

‡Presently at University of California, Los Angeles, California 90024.

§Presently at Niels Bohr Institute, Copenhagen, Denmark.

||U. S. Atomic Energy Commission Contract No. AT(11-1) 1764.

<sup>1</sup>N. K. Glendenning, *Am. Rev. Nucl. Sci.* **13**, 191 (1963).

<sup>2</sup>R. Broglia, O. Hansen, and C. Riedel, in *Advances on Nuclear Physics*, edited by M. Baranger and E. Vogt (to be published).

<sup>3</sup>G. J. Igo, P. D. Barnes, E. R. Flynn, and D. D. Armstrong, *Phys. Rev.* **177**, 1831 (1969).

<sup>4</sup>W. C. Parkinson, D. L. Hendrie, H. H. Duhm, J. Mahoney, J. Saudinos, and G. R. Satchler, *Phys. Rev.* **178**, 1976 (1969).

<sup>5</sup>C. A. Whitten, Jr., N. Stein, G. E. Holland, and D. A. Bromley (to be published).

<sup>6</sup>E. R. Flynn, G. Igo, P. D. Barnes, and D. Kovar, *Phys. Rev. Letters* **22**, 142 (1969).

<sup>7</sup>J. H. Bjerregaard, O. Hansen, O. Nathan, L. Vistisen, R. Chapman, and S. Hinds, *Nucl. Phys.* **A113**, 484 (1968).

<sup>8</sup>E. R. Flynn, D. D. Armstrong, J. Beery, and A. G. Blair, *Phys. Rev.* **182**, 1113 (1969).

<sup>9</sup>J. Borggren, B. Elbek, and L. P. Nielsen, *Nucl. Instr. Methods* **24**, 1 (1963).

<sup>10</sup>D. D. Armstrong, J. G. Beery, E. R. Flynn, W. S.

Hall, P. W. Keaton, and M. P. Kellogg, *Nucl. Instr. Methods* **70**, 69 (1969).

<sup>11</sup>J. C. Hafele, E. R. Flynn, and A. G. Blair, *Phys. Rev.* **155**, 1238 (1967).

<sup>12</sup>C. M. Lederer, J. M. Hollander, and I. Perlman, *Table of Isotopes* (John Wiley & Sons, Inc., New York, 1967), 6th ed.

<sup>13</sup>F. G. Perey, *Phys. Rev.* **131**, 745 (1963).

<sup>14</sup>B. F. Bayman and A. Kallio, *Phys. Rev.* **156**, 1121 (1967); B. F. Bayman, TWOPAR (unpublished).

<sup>15</sup>The  $2p-1h$  states are labeled by  $(n, \alpha, \lambda; j; JM)$  where  $n$  is the number of phonons,  $\alpha$  the particle number ( $\alpha=0, \pm 2$ ), and  $\lambda$  the multipolarity of the phonon.  $j$  denotes the single-particle quantum number [see also D. Bes and R. Broglia, preceding paper, *Phys. Rev. C* **3**, 2349 (1971)].

<sup>16</sup>B. Mottelson, *J. Phys. Soc. Japan Suppl.* **24**, 639 (1968).

<sup>17</sup>Bes and Broglia, Ref. 15.

<sup>18</sup>E. R. Flynn and O. Hansen, *Phys. Letters* **31B**, 135 (1970).

<sup>19</sup>C. Ellegaard, P. D. Barnes, G. Igo, and E. R. Flynn, *Bull. Am. Phys. Soc.* **14**, 1220 (1969); and to be published.

<sup>20</sup>P. D. Barnes, G. Igo, E. R. Flynn, and D. D. Armstrong (to be published).

<sup>21</sup>G. Igo, E. R. Flynn, B. J. Dropesky, and P. D. Barnes, *Phys. Rev. C* **3**, 349 (1971).

<sup>22</sup>D. Kovar, W. D. Callender, C. Maguire, L. J. McVay, and W. D. Metz, *Bull. Am. Phys. Soc.* **14**, 1202 (1969).

<sup>23</sup>C. Ellegaard, J. Kantele, and P. Vedelsby, *Nucl.*

Phys. A129, 113 (1969).

<sup>24</sup>A. F. Jeans, W. Darcy, W. G. Davies, K. N. Jones, and P. K. Smith, Nucl. Phys. A128, 224 (1969).

<sup>25</sup>A. Bohr, in *Proceedings of the International Symposium on Nuclear Structure, Dubna, 1968* (International Atomic Energy Agency, Vienna, Austria, 1969), p. 169.

PHYSICAL REVIEW C

VOLUME 3, NUMBER 6

JUNE 1971

## Effective Operators and the Analysis of Single-Nucleon Transfer Reactions on Closed-Shell Nuclei\*

D. R. Bes and R. A. Broglia†

*University of Minnesota, School of Physics, Minneapolis, Minnesota 55455  
and Los Alamos Scientific Laboratory, University of California, Los Alamos, New Mexico 87544  
(Received 12 October 1970)*

Spectroscopic factors for the one-body stripping and pickup reactions on <sup>208</sup>Pb are analyzed within the particle-vibration-coupling model that was developed in the first paper of this series. The calculation of the transfer amplitudes is performed up to third-order perturbation theory. A comparison with recent experimental data is carried out.

### I. INTRODUCTION

In the last few years it has become more apparent that realizations of concepts such as closed-shell or single-particle states are nowhere found in the Periodic Table, in the sense of the extreme single-particle description.<sup>1</sup> This has been the outcome of improvements in the experimental techniques resulting from the new accelerators. Both one-particle stripping and pickup reactions have been most useful in learning about the distribution of single-particle strength as well as about ground-state correlations or, as usually called in these kinds of experiments, "core excitations." Good examples of the above statements are provided by the systematic experimental information<sup>2</sup> obtained on the  $f_{7/2}$  nuclei; in particular, on the Ca isotopes. The interpretation of the data is usually simpler for double-closed-shell targets (such as <sup>40</sup>Ca or <sup>48</sup>Ca).

Definite theoretical problems have to be solved before the experimental cross sections can be interpreted as single-particle strengths. The three most important problems are:

(1) The extraction of spectroscopic factors from the measured cross sections. This is customarily done in the distorted-wave Born approximation (DWBA), using the separation-energy prescription to calculate the radial form factor. Although the DWBA seems to be a rather successful way of extracting spectroscopic information from nuclear reactions, the separation-energy prescription has little justification and may introduce considerable uncertainty in the spectroscopic factor associated with weak transitions.

(2) The extraction, through the spectroscopic fac-

tors, of quantitative information on both the single-particle states and their admixtures with more complicated states (usually called nonpickup or nonstripping components). For this one needs a good description of the final excited states in the odd nucleus, which depend on the description of the low-lying collective states of the closed-shell system. These states are not necessarily in the system  $N_0$ . If pairing modes are considered, they would include states of the  $N_0 \pm 2$  nuclei. It is easy to see that this problem implies a requirement of self-consistency. At the same time, the modification of the single-particle states due to their coupling to the collective states of  $N_0$  nucleons implies that effective transfer operators should be used. These operators are related to the reaction cross sections as the effective energy matrix elements are to the energy.

(3) If two-step processes are included,<sup>3</sup> the two problems listed above are intimately related and cannot be treated separately.

Some of these problems have been considered by Hamamoto,<sup>4</sup> based on the perturbation treatment of particle vibration suggested by Mottelson.<sup>5</sup>

In this paper we present, following Refs. 4 and 5, a systematic way of dealing with problem 2, concerning both the final-state wave functions and the use of effective transfer operators. Problem 1 will be discussed elsewhere<sup>6</sup> using the approach presented in the work of Ibarra and Bayman.<sup>7</sup> The basis of the model to be used was discussed in an earlier paper.<sup>8</sup> Though the methods described below apply to any closed-shell system, we concentrate our attention on the case of single-neutron stripping and pickup on <sup>208</sup>Pb.

In Sec. II, the description of the  $N_0 \pm 1$  states